EVALUATION OF MULTI-PHASE HEAT TRANSFER AND DROPLET EVAPORATION IN PETROLEUM CRACKING FLOWS*

S. L. Chang, S. A. Lottes, and M. Petrick

Argonne National Laboratory
Argonne, IL 60439
and

C. Q. Zhou
Purdue University Calumet
Hammond, IN 46323

April 1996

*Work supported by U.S. Department of Energy, Assistant Secretary for Fossil Energy, under Contract W-31-109-ENG-38.

To be submitted to 1996 International Mechanical Engineering Congress and Exposition, Nov. 17-22, 1996, Atlanta, GA, sponsored by ASME, Heat Transfer Division.

DISCLAIMER

EVALUATION OF MULTI-PHASE HEAT TRANSFER AND DROPLET EVAPORATION IN PETROLEUM CRACKING FLOWS*

S. L. Chang, S. A. Lottes, and M. Petrick

Argonne National Laboratory
Argonne, IL 60439
and
C. Q. Zhou
Purdue University Calumet
Hammond, IN 46323

ABSTRACT

A computer code ICRKFLO was used to simulate the multi-phase reacting flow of fluidized catalytic cracking (FCC) riser reactors. The simulation provided a fundamental understanding of the hydrodynamics and heat transfer processes in an FCC riser reactor, critical to the development of a new high performance unit. The code was able to make predictions that are in good agreement with available pilot-scale test data. Computational results indicate that the heat transfer and droplet evaporation processes have a significant impact on the performance of a pilot-scale FCC unit. The impact could become even greater on scale-up units.

INTRODUCTION

The commercial-scale fluid catalytic cracking (FCC) system was first introduced in early 1940's. Since then, the FCC process has been constantly improved and become the key conversion process in the modern refinery industry. Over the course of process improvement, cracking reaction time of an FCC unit becomes much shorter and hydrodynamic effects on cracking processes become more apparent. In reviewing the history of FCC process improvement, Bienstock and et al. (1993) indicated that fundamental understanding of the hydrodynamics and heat transfer in the injection zone and riser is critical to the development of a new high performance FCC unit. Under a Corporate Research And Development Agreement (CRADA), Argonne National Laboratory (ANL) conducted a research project in collaboration with the petroleum industry for the development of advanced heavy oil thermal cracking units. Computer simulation and experimental testing were performed to investigate the cracking flow characteristics in the riser

*Work supported by U.S. Department of Energy, Assistant Secretary for Fossil Energy, under Contract W-31-109-ENG-38.

section of the thermal cracking unit. The testing facility was a pilot-scale, 1-barrel-per-day (BPD) thermal cracking unit. One of ANL's computational fluid dynamic (CFD) computer codes, ICRKFLO, was used for this investigation.

Computer codes have been used in the past for modeling portions of the kinetics or hydrodynamic processes in riser reactors. Weekman and Nace (1970) used a 3-lump (oil, gasoline, and dry gas) cracking kinetic model to predict gasoline production in an FCC unit. Dave and et al. (1993) expanded the model and included an additional coke lump in the simulation to predict the coking of the heavy oil cracking processes. Pita and Sundaresan (1991) investigated gas-particle flow patterns in a vertical riser. Theologos and Markatos (1993) used Weekman's 3-lump kinetic model in their two-phase flow calculation of an FCC riser. In a thermal cracking riser, interfacial momentum, heat, and mass transfer processes are the key processes which govern the performance of the flow in the riser. Chang and et al. (1995) developed the ICRKFLO code to simulate a realistic riser flow in an FCC unit by including all three phases of the flow, with models governing heat carrier particle transport, feed oil droplet transport, vaporization of the feed oil droplets, cracking of the feed oil, and coke formation and deposition on heat carrier particles.

The ICRKFLO code was developed by expanding and enhancing an existing two phase reacting flow computer code. The computer code was originally a general computational fluid dynamic code, which numerically solved conservation equations of mass, momentum, and energy for two-phase flows (gas/liquid or gas/solid). It had been successfully used to predict characteristics of two-phase reacting flows in coal-fired combustors (Chang and Lottes, 1993), air-breathing jet engines (Zhou and Chiu, 1983), and internal combustion engines (Chang and Wang, 1987). The code was constantly validated by comparing computational results with available experimental data (Lottes and Chang, 1991 and Chang et al., 1993). For simulating an FCC riser flow, new features were added to the code to model the complex interactions in a three-phase flowfield comprising a carrier gas and droplet and particulate condensed phases. The newly developed computer code was used to predict flow characteristics of a pilot-scale (1 BPD) and a large-scale (10,000 BPD) heavy oil thermal cracking riser unit.

TECHNICAL APPROACH

A schematic of the pilot-scale riser reactor is shown in Fig. 1. Heat carrier particles enter the riser from one side of the tube near the bottom and are lifted by inert gas injected from the center of the riser bottom. In general, the momentum imparted to the particles through drag by the lift is sufficient to lift them into and somewhat beyond the mixing zone surrounding the feed oil injection port in opposition to the gravity force. Feed oil is injected above the particle inlet from the opposite side of the riser tube so the oil droplets can be heated by the particles to induce vaporization. Expansion in the gas phase due to the vaporization process generates additional gas phase momentum which is sufficient to lift the entire flow of particles, vaporizing droplets, and gas with cracked petroleum products up and out of the riser. The interfacial drag, heat transfer, and droplet vaporization processes have a great impact on the performance of a riser reactor. A Cartesian coordinate system is assigned to the riser system with its origin at the lower right corner, an x axis along the tube from bottom up, and a y axis across the tube from right to left.

ICRKFLO uses a combination of fundamental governing conservation equations of physics and models for interphase exchange that use both fundamental physics and engineering correlations to characterize the interphase exchange processes to simulate the riser flow.

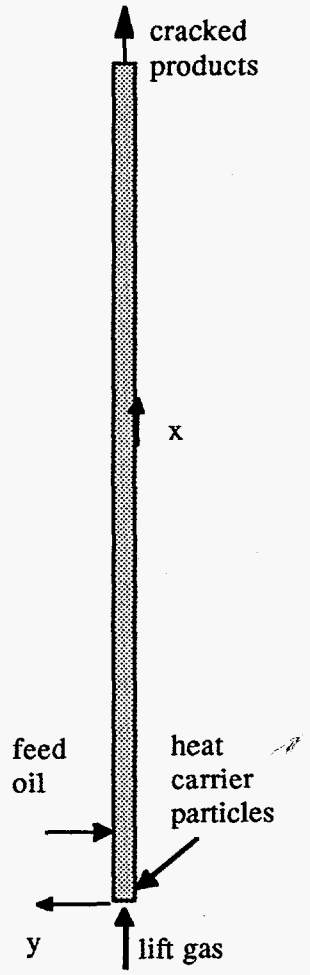

Fig. 1. Heavy Oil Thermal Cracking Riser

Governing Equations

ICRKFLO solves conservation equations of general flow properties for three phases: gaseous species, liquid droplets, and solid particles. General conservation laws, expressed by elliptic-type partial differential equations, are used in conjunction with rate equations governing the mass, momentum, enthalpy, and species for a three-phase flow with gas species, liquid droplets, and solid particles. The governing equations described in this section are derived for the FCC riser flow environment. For convenience in numerical formulation, the governing transport/ conservation equations for the gas phase are put in a common form, Eq.(1):

$$\frac{\partial}{\partial x}(\theta \rho u \xi - \Gamma_\xi \frac{\partial \xi}{\partial x}) + \frac{\partial}{\partial y}(\theta \rho v \xi - \Gamma_\xi \frac{\partial \xi}{\partial y}) = S_\xi \qquad (1)$$

in which ξ is a general flow property, x and y are coordinates, θ is gas volume fraction, u,v are velocity components, Γ is effective diffusivity (calculated from both laminar and turbulent viscosities and an appropriate nondimensional scaling factor), and S_ξ is the sum of source terms.

The liquid and particle phase formulations are based on an Eulerian model. In this formulation, the liquid or particle-phase state of the flow is governed by the elliptic partial differential equations of fluid mechanics, including conservation of droplet and particle number density, momentum, and energy. Liquid droplets in a spray have a spectrum of droplet sizes. To compute droplet properties in a droplet size distribution, droplets need to be divided into size groups, which is a discretization of the droplet size spectrum, and for each size group, droplet properties are determined by solving the governing equations.

Experiments show that droplets have a non-uniform size distribution in a spray. For a typical spray, an exponential function is usually used to describe the droplet size distribution. A droplet number density distribution function $g_s(r)$ is defined as Eq.(2).

$$g_s(r) = br^c \exp(-ar^d) \qquad (2)$$

The droplet number density distribution function employs 4 parameters a, b, c, and d. Two of the parameters are related to the total number density and mean radius and the other two need to be determined empirically. Once empirical parameters c and d are set (a value of 4 is frequently used for both c and d, but they can be easily changed for particular applications) parameters a and b can be expressed in terms of the total droplet number density n_o and the volume mean radius r_m.

$$\frac{g_s r_m}{n_o} = 5.2\ (r/r_m)^4 \exp[-1.14\ (r/r_m)^4] \qquad (3)$$

Equation (3) shows the droplet number density distribution function usually used in the ICRKFLO code expressed in a dimensionless form. The droplet number density distribution function is represented by a solid line in Fig. 2. It is a typical bell-shaped distribution. As the droplet radius increases, the number density function increases from zero at zero radius to a peak ($g = 1.66\ n_o/r_m$) at a radius $r = 0.97\ r_m$ and decreases afterward. Empirical constants c and d are used to adjust the width of the distribution for matching experimental data, when data is available.

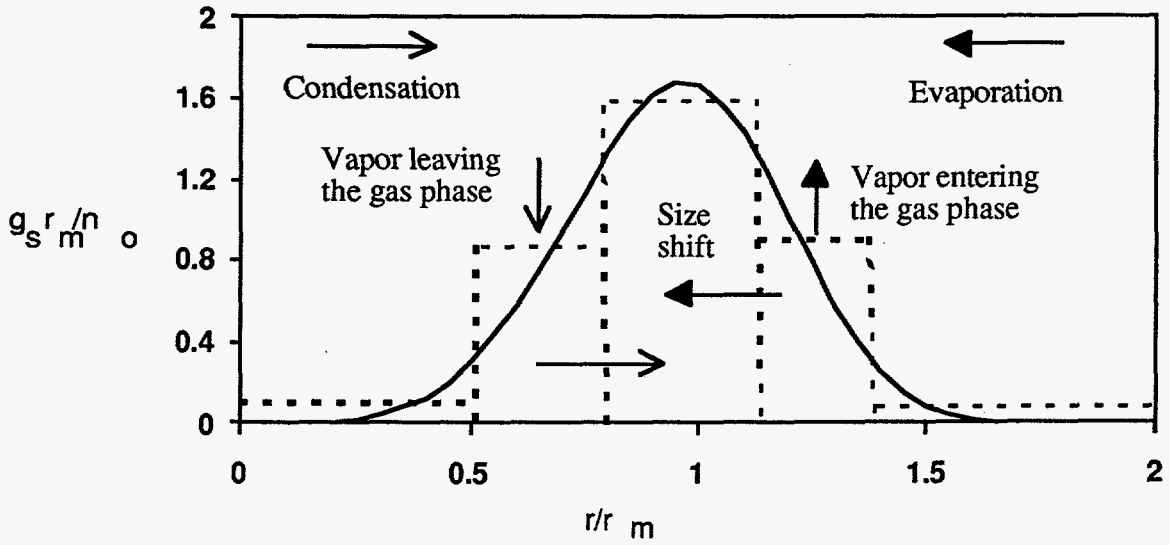

Fig. 2. Droplet Number Density Distribution Function

In numerical calculations, the droplet size distribution function is simplified by lumping droplets into size groups. A 5-lump droplet number density distribution is shown in Fig. 2, represented by the dashed line rectangles. The arrows indicate the effects of the evaporation and condensation processes. Vaporization causes droplets to shift from larger to smaller size groups at a computed rate and also results in deposition of vapor from the droplets into the gas phase.

Similar to the gas phase formulation, the governing transport equations for the liquid and particle phases are put in a common form, Eq.(4).

$$\frac{\partial}{\partial x}(n_k u_{c,k}\xi - \Gamma_\xi \frac{\partial n_k \xi}{\partial x}) + \frac{\partial}{\partial y}(n_k v_{c,k}\xi - \Gamma_\xi \frac{\partial n_k \xi}{\partial y}) = S_\xi \qquad (4)$$

in which n_k is droplet or particle number density of kth size group, $u_{c,k}$ and $v_{c,k}$ are droplet or particle velocity components of kth size group in the x and y direction respectively, Γ is droplet or particle diffusivity resulting from interaction with turbulence in the gas phase, and S_ξ is the sum of source terms. Although the formulation and computer code allow for a size spectrum of both droplets and particles, in this study only one size of group of particles was used. A size spectrum of droplets was used however, and that size distribution does have a significant effect on the computed results because vaporization rates, drag effects, and dispersion of droplets by gas phase turbulence are all functions of droplet size.

Table I lists source terms for each of the properties of the condensed phases, noting the applicable governing equation. Each property has a transport equation for each size group, k, and the source terms must be computed for each of the size groups.

Table I. Source Term List for Condensed Phase Flow Transport Equations (Size Group K)

ξ	Transport Equation	Source Term
1	droplet number density	evaporation rate (size spectrum shift rate)
1	particle number density	0
$u_{c,k}$	x-momentum	interfacial drag, gravitational body force
$v_{c,k}$	y-momentum	interfacial drag, gravitational body force
$T_{c,k}$	energy	heat transfer between phases
d_c	coke mass fraction (particle phase)	heavy oil cracking reactions

Phenomenological Models

Phenomenological models are used to define the diffusivity and source terms of the governing equations. ICRKFLO uses 5 major phenomenological models: lumped integral reaction, coke interphase transfer and transport, two-parameter turbulence, interfacial drag and heat transfer, and droplet dispersion and evaporation models. The primary interfacial transfer models for momentum, heat, and mass that greatly influence development of flow patterns and cracking processes in an FCC riser are presented in the following sections.

Interfacial Drag Model

A gas flow is generally driven by a pressure gradient and a particle/droplet flow is driven by the drag force from the gas flow. The drag force is caused by the velocity difference between the gas and solid phases (called slip velocity, with components u_δ,v_δ).

Empirical equations are commonly used to correlate the drag force with the slip velocity. Drag force is a vector defined by two orthogonal components: one in the x-direction and the other in the y-direction. Since the derivation of the two components are in parallel, only the derivation of the x-component will be presented in the following. For a single droplet or particle in the gas, the x-direction drag force ($F_{d,x}$) of gas exerted on the droplet or particle can be expressed as a function of the slip velocity kinetic energy $\rho u_\delta^2/2$, droplet or particle cross-sectional area πr^2, and an empirical coefficient C_d as shown in Eq.(5). The droplet or particle drag force is in the same direction as the slip velocity. When the slip velocity is positive, the drag force is positive. When the slip velocity is negative, the drag force is negative.

$$F_{d,x} = \frac{1}{2}\rho |u_\delta| u_\delta \pi r^2 C_d \tag{5}$$

The drag coefficient Eq.(6) includes two major effects on the drag force, one is viscous, based on a correlation using a Reynolds number Re_s, defined using slip velocity, and the other is the evaporation effect represented by a transfer number B, Eq.(8). In Eq.(8), L is the latent heat of a droplet and T_b is the boiling temperature of a droplet. When droplet temperature is less than its boiling temperature, there is no significant evaporation, the transfer number is zero, and the drag force depends on the viscous effect alone.

$$C_d = \frac{24}{Re_s}\frac{(1+0.15Re_s^{0.687})}{1+B} \tag{6}$$

in which,

$$Re_s = \frac{2\rho |u_\delta| r}{\mu} \tag{7}$$

and

$$B = \begin{cases} \dfrac{C_p(T_s - T_b)}{L} & \text{if } T_s \geq T_b \\ 0 & \text{if } T_s < T_b \end{cases} \tag{8}$$

Interfacial Heat Transfer Model

Empirical equations are also used to correlate the interfacial heat transfer with the slip velocity. For a single particle or droplet in the gas, the heat transfer between the gas and the particle or droplet is expressed as,

$$q_s = 2\pi r \lambda Nu_s (T - T_s)\delta(T_b) \tag{9}$$

in which, λ is thermal conductivity of the gas, Nu_S is an empirical Nusselt formula, (Eq. 10), and $\delta(T_b)$ is a step function, which changes from one to zero when a droplet or particle reaches its phase change temperature. The Nusselt formula (Eq. 10) includes two major effects of the interfacial heat exchange, one is the momentum effect represented by the Reynolds number Re_S, Eq.(7), and the other is the diffusivity effect represented by the Schmidt number Sc, Eq.(11). In Eq.(11), D is the mass diffusivity of a species. After the droplet temperature reaches the boiling temperature further heat transfer from the gas to particles goes into droplet evaporation. In this case, the step function $\delta(T_b)$ makes q_S zero for T_S equal to T_b.

$$Nu_s = 1 + 0.276\, Re_s^{1/2}\, Sc^{1/3} \tag{10}$$

$$Sc = \frac{\mu}{\rho D} \tag{11}$$

Droplet Evaporation Model

The source term in the gas continuity equation is the evaporation rate of the droplets per unit volume. By necessity, droplet state and droplet processes in a macro scale simulation must be treated statistically. The computation of evaporation of hundreds of thousands or even millions of individual droplets in the system in detail, based on their local environment and individual composition and state, is simply impossible with even the fastest existing computing equipment, and that approach will remain unattainable for the foreseeable future. The droplet evaporation model, therefore, is based on the fundamental physics of stationary single droplet evaporation and then modified for large groups of droplets in a convective environment using correlations. Direct interactions between droplets (collisions) are ignored, however, droplets do interact with each

other indirectly through their effects on the gas phase. As noted previously, the current state of the droplet modeling in the ICRKFLO computer code treats droplets with an Eulerian approach and does include modeling of an evolving size spectrum of droplets with transportable properties that are a function of droplet size. Because gas phase properties, such as specific heat, heat transfer coefficients, etc. may be functions of local gas phase properties, different size droplets will respond differently to varying local conditions because the correlations used are functions of droplet size. The evaporation model is characterized briefly as follows. The classical solution giving the droplet evaporation rate for a single stationary droplet is (Williams, 1985),

$$(\frac{dm}{dt})_{stat} = 4\pi r(\lambda / C_p)\ln(1+B) \tag{12}$$

A correction for the convection effect, sometimes referred to as the Ranz-Marshall model (Aggarwal, et al., 1984) can be applied to the stationary solution Eq.(12) to yield an empirical correlation for vaporization in a flow. The correction adds a Nusselt number Nu_s to the stationary solution.

$$(\frac{dm}{dt})_{conv} = 4\pi r(\lambda / C_p)\ln(1+B)Nu_s \tag{13}$$

The total evaporation rate at a point per unit volume of physical space is determined by integrating the product of single droplet evaporation rate and the spray distribution function over the droplet size spectrum. The droplet evaporation also changes the momentum of gas flow. Droplet momentum is assumed to be maintained as the droplets change phase. Therefore, as droplets vaporize, part of the original droplet momentum is added to the gas flow for the droplet vapor via source terms in the gas phase momentum equations .

NUMERICAL SCHEME

Computational Grid

ICRKFLO was used to investigate heat transfer patterns and flow characteristics in a heavy oil cracking riser. A simple schematic of the riser is illustrated in Fig. 1. Riser dimensions are proprietary information of a petroleum company and will not be discussed here. A computational grid system was defined containing two zones: a mixing zone and a reaction zone. The mixing

zone is in the bottom section where carrier particles, oil droplets, and lift gas mix and a significant amount of droplet vaporization takes place as determined by the mixing process. The reaction zone is the rest of the riser where heavy oil vapor is cracked into light oil vapor, dry gas, and coke. Since a more complex flow pattern is expected in the mixing zone, a finer grained grid cell structure is defined in this zone. Grid lines are especially closely spaced at the entry ports for the heat carrier particles and the heavy oil droplets. In order to conserve computational time and still provide adequately accurate results, a grid sensitivity study was conducted to choose a grid system that uses as few cells as possible (approximately 1000 scalar cells) while yielding stable numerical results to approximately three decimal digits upon further grid refinement. An important feature of the control volume approach used in the ICRKFLO code is that it is conservative in terms of mass, energy, species, and all variables solved for via the transport equations, both locally and globally to a very high degree (see Numerical Convergence section) regardless of grid size. This feature helps to ensure that results are physically realistic regardless of grid size and that trends in parametric studies are relatively independent of grid size even for relatively coarse grids. Little would be gained therefore in attempting to refine the grid to make results grid independent to more than 3 or 4 decimal digits.

Numerical Convergence

The ICRKFLO code was set up to calculate flow properties in the riser with the processes of mixing, heat transfer, vaporization, and cracking (including coke formation and deposition on carrier particles). The calculation includes four gas species in the gas phase, three droplet size groups in liquid phase, a single particle size group, and a coke species in the solid phase. The computer code calculates flow properties of three phases in all computational cells. Obtaining a converged solution of a set of non-linear particle differential equations is always difficult. In this computer code, a calculation is considered a converged solution if the local and global mass balances of the three phases are smaller than a set of pre-determined criteria. For these simulations, convergence criteria defined by average mass residual of all computational cells are 10^{-10} (in dimensionless form and normalized by the inlet mass flow rate) for gas phase and 10^{-8} for both liquid and solid phases. Besides, the average and maximum relative residuals for all

transport equations are also checked to ensure that they are sufficiently small before the run is accepted as truly converged and ready for post processing of generated result data. Generally in this application, with reasonable boundary conditions (inlet flow rates, etc.), a converged solution can be obtained in about 3000 numerical iterations for gas, liquid and solid phases as shown in Fig. 3. On a 486/66 personal computer with 16 megabytes of random access memory, using a 32-bit FORTRAN compiler, this computation takes about 12 hours.

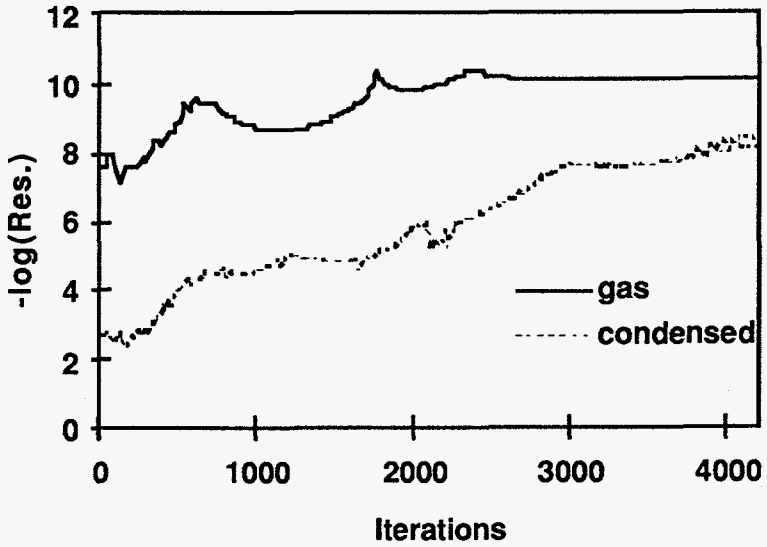

Fig. 3. Gas and Condensed Phase Mass Residuals

RESULTS AND DISCUSSION

Pilot-Scale Riser

Baseline Results

A test run on the pilot plant was chosen as the baseline case. Chang and Lottes (1995) used the baseline test data and determined local temperature dependent kinetic constants for the lumped reaction model. Using the reaction model, calculations were made for several riser flow cases. Computational results were compared with the experiments, confirming a close match in overall pressure drop, temperature change, and product yields. These results verified that the detailed modeling in the computer code could predict the overall macroscopic behavior of the riser flow. Results pertaining to the pressure drop and temperature will be presented in the following discussion, however, most of the discussion will focus on the details of processes in the mixing

and vaporization zone of the riser (about one tenth of the riser length) because this region is where most of the significant interfacial exchange of momentum, heat, and mass takes place.

Pressure is nearly uniform across the riser, and the development of pressure drop up the riser length is shown in Fig. 4. Gas pressure drops rapidly in the mixing zone where number densities are high and there are significant drag effects for turning the particles into the downstream. The pressure continues to drop at a slower pace in the reaction zone where heavy oil vapor is converted into lighter components. The normalized computed pressure drop shows good agreement with the measured value (represented by a square in the figure). This agreement is within the range of experimental error and indicates that the complex set of modeled processes in the riser which affect pressure represent the physics of those modeled processes fairly well.

Figure 5 shows the development of gas density up the riser. Density increases rapidly in the mixing zone because of the additional gaseous species resulting from the vaporization of the oil droplets. The asymmetry over a riser cross section is a consequence of injecting heat carrier particles from one side and feed oil from the other. In spite of the large aspect ratio of the pilot-scale riser this asymmetry is seen to persist in the density profile to some extent over the entire riser length.

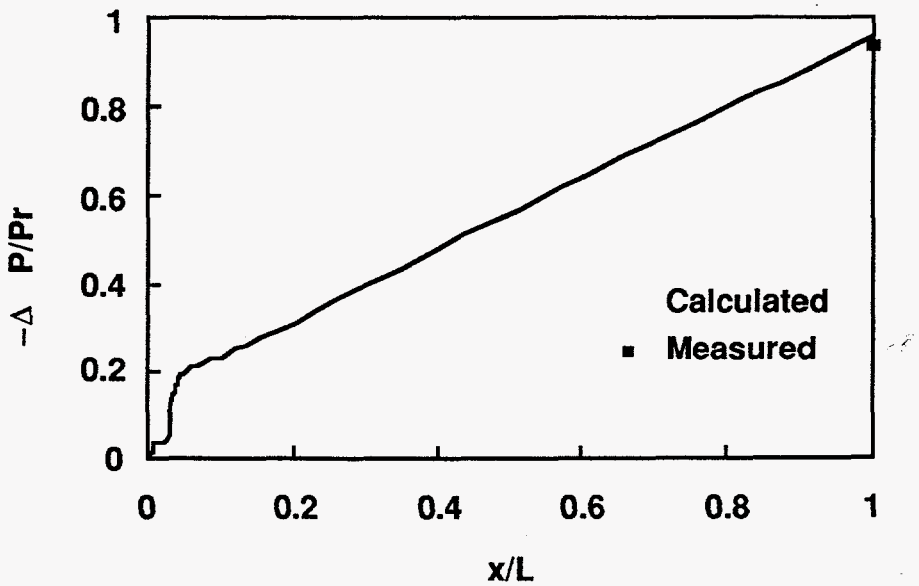

Fig. 4. Development of Pressure Drop up the Riser

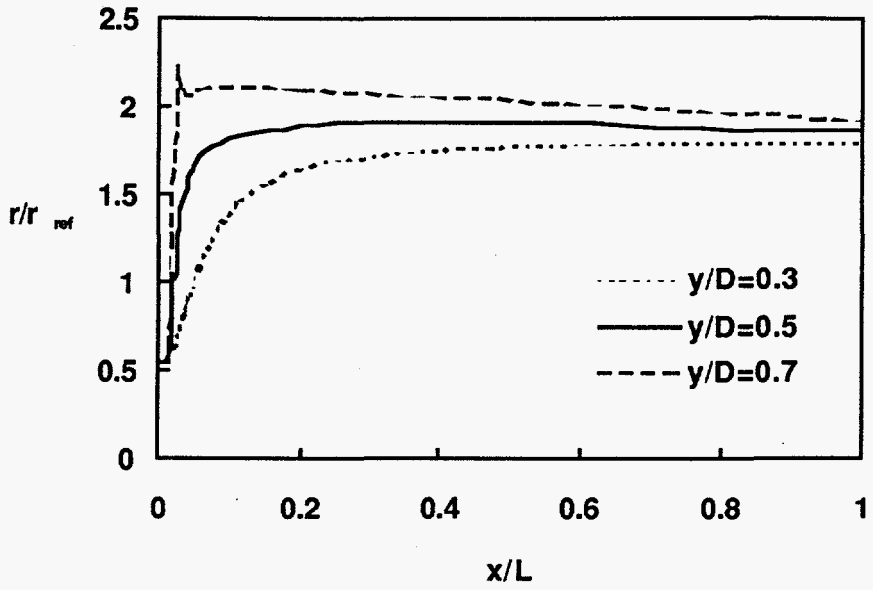

Fig. 5. Development of Density Up the Riser

Figure 6 shows the development of gas temperature up the riser. The gas temperature is strongly influenced by the heat transferred from the particles to the gas and the heat required to vaporize the heavy oil droplets. Average gas temperatures at three locations, i.e., inlet, zone 1, and exit, show good agreement with measured values (within the range of experimental measurement error). The close agreement in the available data show that the detailed heat transfer computations among the phases are capable of predicting the temperature at two downstream points in the riser, and this result indicates that the detailed models do characterize the primary physical processes of heat transfer among phases with reasonable accuracy and therefore the predicted trends in local effects in the flowfield are also reasonable characterizations of the trends and flowfield patterns occurring in an actual riser when parameters, such as injection angles, mass flow rates, etc., are varied. The variation of gas temperature at a riser cross section is a function of local particle and droplet number density and temperature, vaporization rates, residence time, and upstream history.

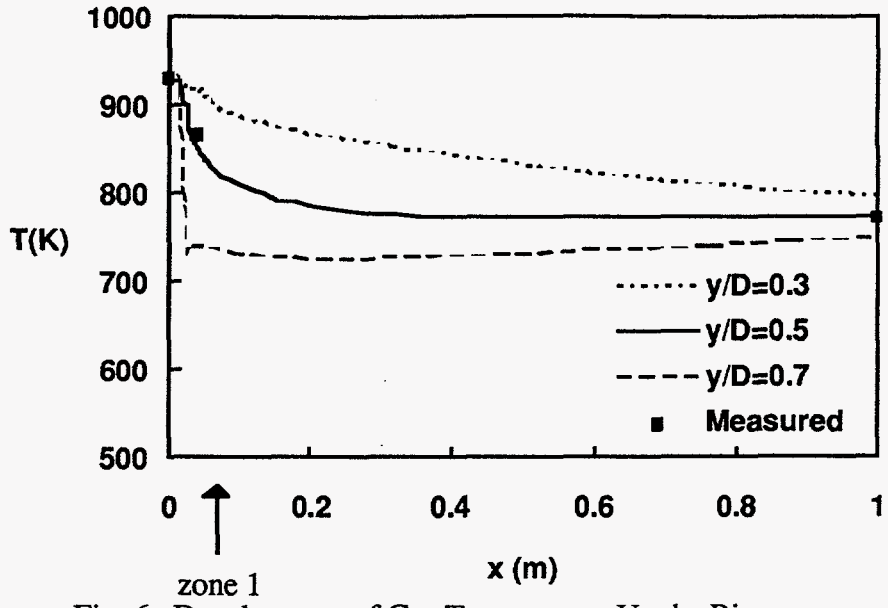

Fig. 6. Development of Gas Temperature Up the Riser

Droplet Evaporation

The primary mixing zone of the riser reactor is from inert gas inlet at the bottom to a few diameters above the feed oil inlet as shown in Fig. 1. In the pilot-scale test facility, the most of the length of the riser tube has a very small diameter, too small for adequate mixing and turning of particles and droplets into the downstream when injected from the side. Therefore, a portion of the mixing zone from the bottom of the riser to a short distance beyond the feed oil injector port has a larger diameter. The change of tube width, the injection of particles, droplets, and gas, the heat transfer between phases, and the vaporization of liquid droplets create a complex multi-dimensional flow pattern in the mixing zone.

Flow patterns for the base case for gas, droplet, and particle velocity and particle and droplet number densities in the mixing zone are plotted in Figs. 7 to 9. The x-axis represents relative position up the length of the riser. The y-axis represents the fraction of the distance across the riser as measured from the particle injection side. The velocity field is plotted as velocity vectors. The vector length is proportional to velocity magnitude. For particles and droplets of the various size groups, contours of droplet or particle number density are also plotted. These contours represent equal number density curves given in number of droplets or particles per unit volume.

The velocity vector field for the gas flow is shown in Fig. 7. The gas velocity field in this mixing zone of the riser is highly influenced by the deposition of new mass in the gas phase from vaporizing heavy oil droplets. The vaporizing droplets cause expansion of the gas and therefore an increase in gas velocity. This phenomenon is seen most clearly in the region just before and into the necking down of the tube. Area change alone is insufficient to account for some of the large velocities computed in this region. Near the lift gas entry, the overwhelming number and mass of the carrier particles entering from the lower left hand corner accelerates the lift gas toward the upper left hand corner of the figure. The heavy oil jet and vapor generated from it are required to turn the carrier particles and lift gas strongly back toward mid stream.

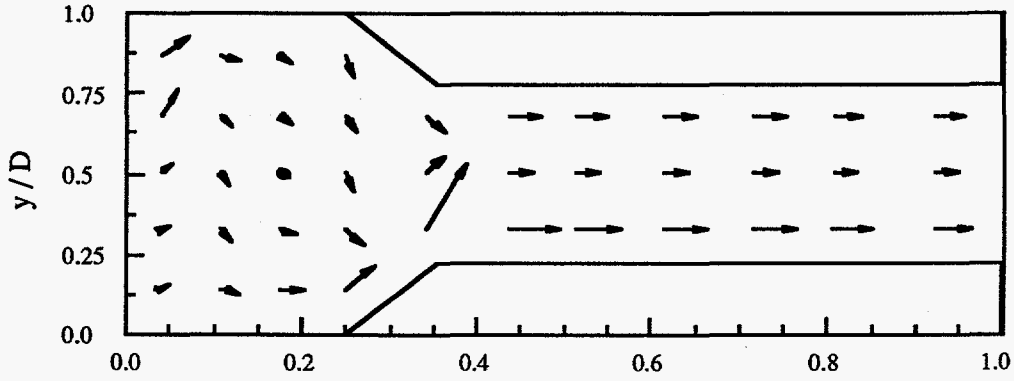

Fig. 7. Gas Velocity in the Mixing Zone

In the simulation, the heavy oil spray is represented by droplets of three size groups. Figures 8a, 8b, and 8c show the velocity and number density field for the small, medium, and large droplet size groups, respectively. In Fig. 8a, most of these droplets are either turned quickly into the downstream because of their small size, or they are vaporized, and consequently droplets of small size are primarily confined to the upper half of the figure, which is the side of the tube containing the oil injection port. Small droplets respond very rapidly to changes in gas velocity, and therefore the velocity vector field for these droplets is very close to that of the gas flow shown in Fig. 7. Mid-sized droplets constitute the size group of highest number density, and therefore also oil mass flow, within the number density distribution of the oil jet. In Fig. 8b, the rapid drop of number density from 300 to 10 #/(unit volume) indicates a fast evaporation rate in the mixing zone.

Because of the heating and vaporization delay, the contour line of 10 #/(unit volume) can be seen to extend below the centerline of the tube in the figure. Some droplets hit the tube wall and are vaporized on it. The oil jet spray is angled toward the downstream, and the consequent plume is clearly visible in the 200 #/(unit volume) contour. In Fig. 8c, larger droplets show a much slower evaporation rate.

Figure 9 shows a velocity field of the carrier particles significantly different from that of the gas velocity field (in Fig. 7). First, particles move from the inlet port (y/D=0) to the far side (y/D=1) of the tube carried by their inlet momentum and the lift gas. Next, particles are turned back toward mid-stream by the oil spray. Finally, particles are accelerated by the expansion caused by vaporizing oil droplets and flow up the riser. Because of the necking of the tube, particles are forced to move toward the tube center.

In the baseline case, much vaporization of oil occurs near the oil inlet and most of the mid and smaller sized droplets are turned into the downstream before they cross the centerline at y/D = 0.5. Therefore most of the vaporization of oil occurs in the region y/D > 0.5. Because the oil vapor is of high molecular weight compared to the lift gas and vaporization lowers gas temperature, the gas density in the region y/D > 0.5 is greater than in the region y/D < 0.5 in the downstream of the mixing zone shown in the figure.

Scale-up Analysis

A detailed treatment of scale-up analysis is not in the scope of this paper. However, a brief discussion of a scale-up analysis is given here because of the great potential for cost savings that can be realized by doing relatively inexpensive simulations with parametric studies. Such studies make possible optimization of configuration and operating conditions for a full-scale unit before making a large capital investment in a full-scale or several intermediate scale prototype units and then expending much effort and money trying to adjust operating conditions to bring the performance of the scale-up units close to that of the pilot-scale unit. Computations were carried out for several risers having a similar geometry with feed and heat carrier particle injectors on opposing sides, which is necessary for penetration of feed oil and particles into the central regions of large scale-up units.

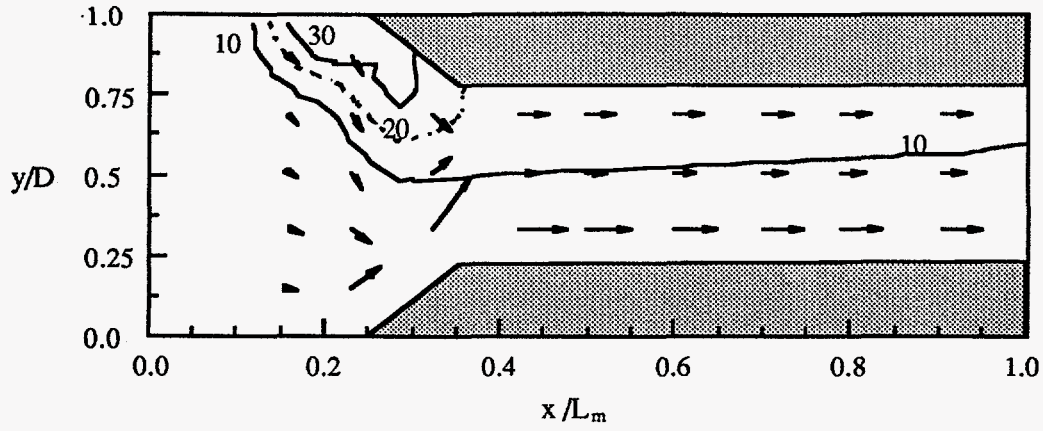

(a) Small Droplets

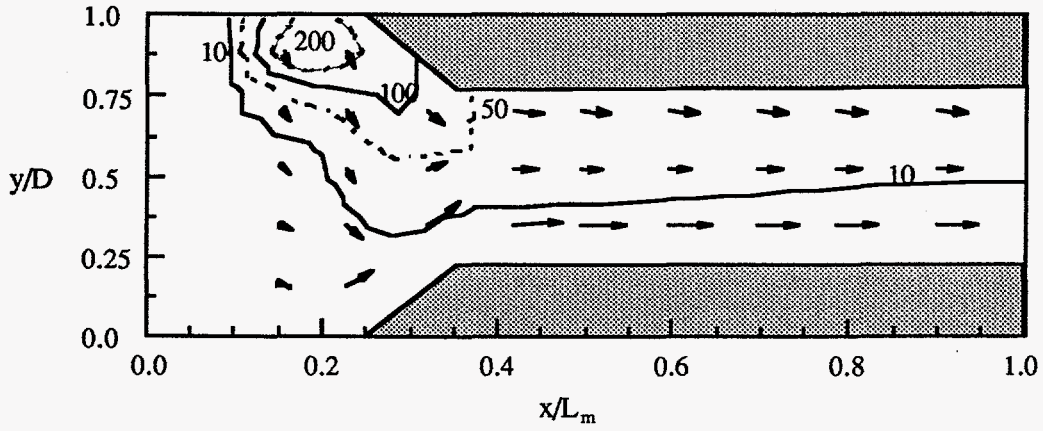

(b) Mid-sized Droplets

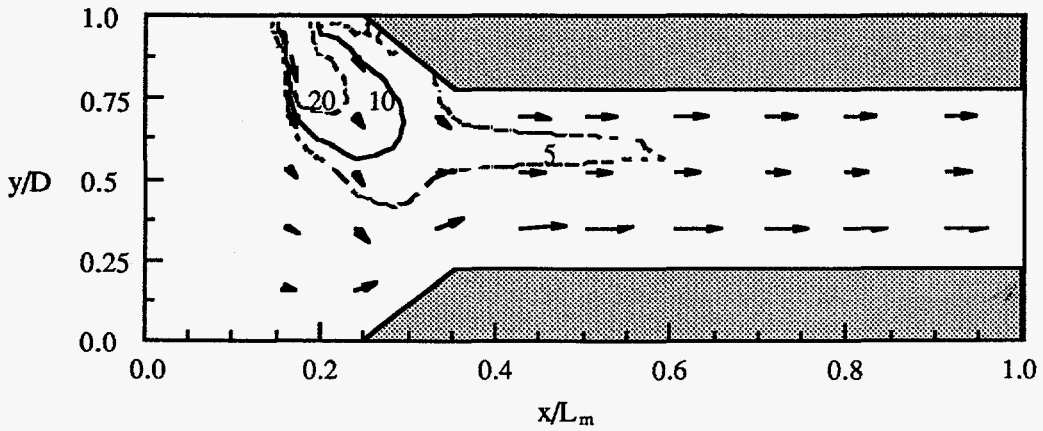

(c) Large Droplets

Fig. 8. Velocity and Number Density field in the Mixing Zone

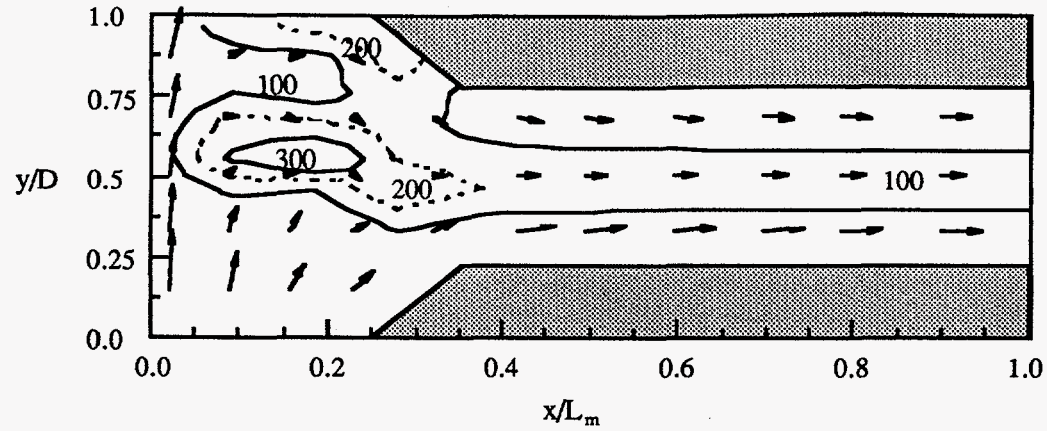

Fig. 9. Particle Velocity Vectors and Number Density Contours in the Mixing Zone

As discussed in the previous section, a pilot-scale riser has a very large aspect ratio, but the aspect ratio of a large production-scale riser is much smaller. This geometry difference results in a number of highly significant scale-up effects. The first and most obvious result of the large change in aspect ratio is that the mixing zone between lift gas, heat carrier particles, and feed oil droplets occupies a significant portion of the scale-up riser height making mixing zone processes much more important in overall riser performance.

Results of production-scale unit simulations show significant differences when compared to pilot-scale simulations. Velocity vectors in the mixing zone for heat carrier particles for a symmetric pilot-scale riser are shown in Fig.10. The particles are turned up the tube by the lift gas and develop rapidly into a fairly uniform upward flow patters after passing the feed oil injectors.

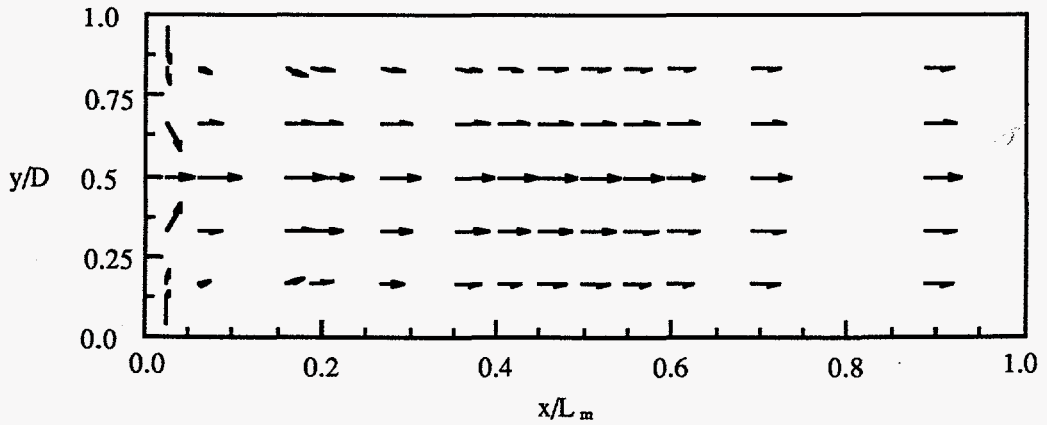

Fig. 10. Particle Velocity Vectors for Symmetric 1 BPD Riser

In contrast to the simple particle flow pattern of the symmetric pilot-scale riser, the heat carrier particle flow pattern for a production-scale unit in the mixing zone is much different and much more complex as shown in Fig. 11. Particle recirculation zones are found in the scaled up unit, with particles falling back down the riser in the near wall zone. The complex flow patterns with recirculation zones for all three phases creates significant cross section non-uniformities over a large fraction of the total riser height, and these non-uniformities in particle and droplet distributions, and consequently temperature distribution affect vaporization, cracking, and ultimately product yields.

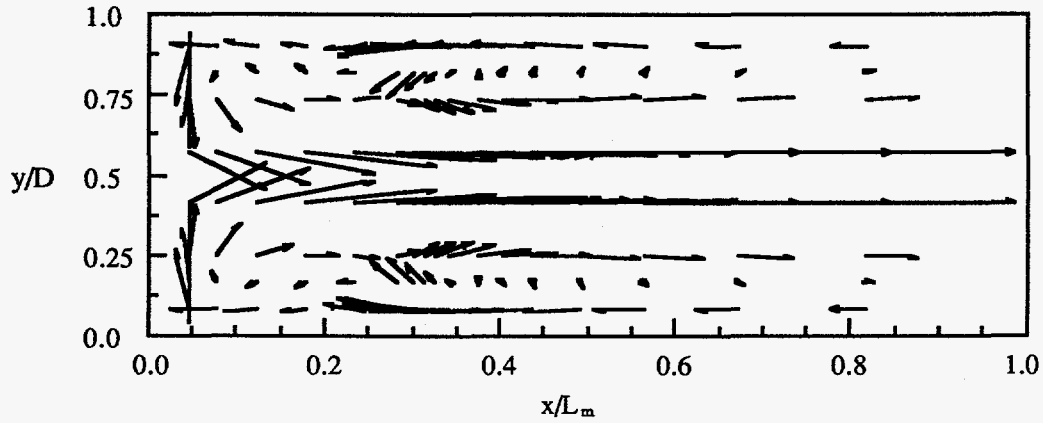

Fig. 11. Particle Velocity Vectors for a Symmetric Production Scale Riser

The computed results indicate that flow patterns and oil cracking processes in the riser unit may change dramatically on scale-up. The failure to preserve aspect ratio is particularly significant because it increases the length of mixing zone of heat carrier particles and oil to a large fraction (approximately in the range of one sixth to one third) of the riser height. The large tube diameter in comparison to particle size of the scale-up riser results in much less turbulent mixing of particles over the cross section and consequently particles in the slower gas flow near the wall fall back down the riser under the influence of gravity. This phenomenon sets up recirculation zones in the lower portion of the riser, and these recirculation zones have a profound effect on the mixing zone flow development, heat transfer, droplet vaporization, and oil cracking, which lead to a significant shift in product yields at the exit. Additional calculations are needed to determine if optimization of the scale-up riser could bring cracking product fraction yields back to approximately those achieved with the pilot-scale riser.

CONCLUSIONS

A new analysis tool has been developed for use in research and development of a heavy oil thermal cracking riser. This tool is a reacting multiphase CFD computer code, named ICRKFLO. The computer code can be used in a cost-effective and time saving manner (for two dimensional computations it can be run on a Pentium(personal computer and reach a highly converged solution in a couple of hours). The overall correctness of ICRKFLO was assured to the extent possible in three ways. First, the code was developed from an existing validated 2-phase reacting flow computer code. Second, all computed results were carefully reviewed for physical reasonableness. Finally, the code was validated by comparing computed results with experiment data conducted on pilot-scale risers.

Computed results have shown good agreement with the available experimental data. The validated code was used to study the detailed internal processes of interphase mixing, momentum, heat, and mass transfer via oil droplet vaporization over a size spectrum in a pilot-scale riser. Results of this study showed that the hydrodynamics of mixing among the phases and interphase exchange rates in the lower portion of the riser play an important role in the initial development of the flow and cracking processes within the riser. Subsequent computational studies showed that the mixing zone performance becomes even more important on scale-up units because of the change in aspect ratio of the riser with consequent large change in internal flow patterns.

ACKNOWLEDGMENTS

This work was supported by U.S. Department of Energy, Assistant Secretary for Fossil Energy, under Contract W-31-109-ENG-38. Ernest Zuech of DOE at Bartlesville Project Office was program manager. Francis Dawson of California Synfuels, Inc. is greatly appreciated for his contribution in analyzing the testing results of a pilot-scale FCC unit.

NOMENCLATURE

a	parameter of particle size distribution
B	transfer number
b	parameter of particle size distribution
c	parameter of particle size distribution
C_d	drag coefficient
C_p	specific heat (J/kg-K)
C_μ	turbulence empirical constant
D	reference diameter (m)
d	parameter of particle size distribution
d_c	coke mass fraction (kg/kg of solid)
F_d	drag force (N/m^2)
g_s	droplet number density distribution function ($\#/m^3$-m)
h	enthalpy (J/kg)
k	turbulent kinetic energy (J/kg)
L	latent heat (J/kg)
L	reference riser length (m)
L_m	reference mixing region length (m)
M_i	molecular weight (kg/kmol)
m_s	particle mass (kg)
n	order of reaction
n_i	droplet or particle number density (number of droplets/m^3)
Nu	Nusselt number
p	pressure (Pa)
q	interfacial heat flux (J/m^3-s)
R	gas constant (J/kmol-K)
r	droplet or particle size (μm)
r_m	mean droplet or particle radius (m)
Re_s	Reynolds number
S	Source term in governing equations
Sc	Schmidt number
T	temperature (K)
t	time (s)
x	x coordinate (m)
y	y coordinate (m)
u	velocity component in the x-direction (m/s)
u'	velocity fluctuation (m/s)
v	velocity component in the y-direction (m/s)

Greek Symbols

δ	slip property
ε	turbulent dissipation rate (J/kg-s)
ϕ	catalyst decay function
θ	void fraction
Γ	effective diffusivity (pa-s)
λ	gas conductivity (J/s-m-K)
λ_t	macro turbulent length scale (m)
μ_t	turbulent viscosity (pa-s)
ξ	general variable for 1, u, v, h, f, k or ε
ρ	density (kg/m^3)

Subscripts

0	reference value
b	boiling property
c	condensed phase (droplet or particle)
d	droplet
k	droplet size group k
s	solid phase
δ	slip property
ξ	general variable

REFERENCES

Aggarwal, S.K., A.Y. Tong, and W.A. Sirignano, "A Comparison of Vaporization Models in Spray Calculations," AIAA Journal 22(10):1448-1457, (1984).

Bienstock, M.G., D.C. Draemel, P.K. Ladwig, R.D. Patel, and P.H. Maher, "A History of FCC Process Improvement Through Technology Development and Application," AIChE Spring National Meeting, Houston, TX, (1993).

Chang, S.L. and S.A. Lottes, "Integral Combustion Simulation of a Turbulent Reacting Flow in a Channel with Cross-Stream Injection," Numerical Heat Transfer Part A, 24(1):25-43 (1993).

Chang, S.L., and C.S. Wang, "Thermal Radiation and Spray Group Combustion in Diesel Engines," ASME Winter Annual Meeting, Boston, Mass., HTD-81:25-34 (December 13-18, 1987).

Chang, S.L., S.A. Lottes, and M. Petrick, "Development of a Three-Phase Reacting Flow Computer Model for Analysis of Petroleum Cracking," Proceedings of 1995 Mid-America Chinese Professional Annual Convention, Itasca, IL, pp. 281-288 (June 23-25, 1995).

Chang, S.L., S.A. Lottes, J.X. Bouillard, and M. Petrick "Study of Multi-Phase Flow Characteristics in an MHD Power Train," Proceedings of 31st Symposium of Engineering Aspects of Magnetohydrodynamics, Whitefish, Montana, pp. Vb.2.1-12 (June 29-July 1, 1993)

Dave, N.C., G.J. Duffy, and P. Udaja, "A Four-Lump Kinetic Model for the Cracking/Coking of Recycled Heavy Oil," Fuel, 72(9):1331-1334, (1993).

Lottes, S.A., and S.L. Chang, "Computer Simulation of Jet Penetration and Fluid Mixing in a Channel with Cross-Stream Jets," Proceedings of the 7th International Conference on Advanced Science and Technology, ANL, IL, pp. 188-198, (1991).

Pita, J.A. and S. Sundaresan, "Gas-Solid Flow in Vertical Tubes," AIChE Journal, 37:1009-1018, (1991).

Theologos, K.N. and N.C. Markatos, "Advanced Modeling of Fluid Catalytic Cracking Riser-Type Reactors," AIChE Journal, 39(6):1007-1017, (1993).

Weekman, V.W. and D.M. Nace, "Kinetics of Catalytic Cracking Selectivity in Fixed, Moving, and Fluid Bed Reactors," AIChE Journal, 16(3):397-404, (1970).

Williams, F.A., "Combustion Theory," Benjamin/Cummings Pub. Co., Inc., (1985).

Zhou, X.Q., and H.H. Chiu, "Spray Group Combustion Processes in Air Breathing Propulsion Combustors," AIAA/SAE/ASME 19th Joint Propulsion Conference, Seattle, Washington, AIAA-83-1323, (1983).